A Feasibility Study of Placing a Heated Turbulence Grid in Front of an Air-Cooled Fuel Cell Stack in Freezing Conditions

Martinho, Diogo Loureiro; Hansen, Jóhannes; Yin, Chungen; Berning, Torsten

Published in:
ECS Transactions

DOI (link to publication from Publisher):
10.1149/10807.0119ecst

Publication date:
2022

Document Version
Accepted author manuscript, peer reviewed version

A Feasibility Study of placing a Heated Turbulence Grid in Front of an Air-Cooled Fuel Cell Stack in Freezing Conditions

Diogo Loureiro Martinho, Jóhannes Hansen, Chungen Yin, Torsten Berning

Department of Energy Technology, Aalborg University, Aalborg, Denmark

This paper aims to better understand the temperature profile of a turbulence inducing grid if pre-heating of the incoming air in the cathode channel is required when the stack is operating under freezing conditions. The goal of this study is to design the grid by changing its thickness and the number of pores. A three-dimensional, steady-state computational fluid dynamic model was developed and validated for a baseline case of a single cathode channel of an air-cooled cell. The computational domain consists of the cathode flow channel, a gas diffusion layer, and the turbulence inducing grid. Four different grid designs were analyzed and compared, and in the best case heating of the turbulence grid was achieved where the temperature of the grid will be 236 ºC and the power consumption will be around 30 % of the total power produced by the fuel cell stack. It is concluded that 2 mm thickness is not sufficient leading to too high temperatures, and a multitude of staggered grids might be required.

Introduction

A fuel cell is an electrochemical device used to convert chemical energy of a fuel, such as hydrogen, into electricity. In and air-cooled fuel cell stack the reactant air is also the coolant which necessitates high stoichiometric flow ratios in the range of 50-100, depending on the ambient temperature (1).

According to a recent study, the fuel cell market is growing due to the demand of new sources of energy to be used in a wide range of portable utilities, unmanned air vehicle, stationary power applications and, finally fuel cells can also be used as the main power source or as a range extenders in the automotive field (2). Within the several different types of fuel cells, the air-cooled proton exchange membrane fuel cell is reliable for applications requiring a few kilowatts due to their simplicity and operating setup which is characterized by the absence of a secondary coolant loop. However, this type of cell has a tremendous drawback regarding the current density that can be drawn, around 0.3-0.4 A/cm^2 (1) (3).

Previous studies proposed the placement of a turbulence inducing grid at the inlet of the cathode to improve the heat transfer inside the cathode channel and enhance the performance of the fuel cell (4). Additionally, different grid types were studied where parameters such as thickness, rib width, pores angle and the distance were varied. It was found the most important variable to achieve a higher performance was the distance between the cathode inlet channel and the turbulence inducing grid where the best

experimental result was at 2.5 mm (5). The results of this study were an increase of 20% with regards to the power density and 30% when looking at the cell voltage.

Afterwards, an attempt to replicate the previous experimental results numerically was done (6). However, the results achieved only pointed out a higher performance of 10.42%. Some assumptions were taken and in order to correct possible inaccuracies of the previous study, a second study was done (7). The research accomplished a lower temperature of the fuel cell when having a turbulence inducing grid before the inlet when it was placed 2 mm away from the inlet which was in very good accord with the experiments.

As air-cooled fuel cells are gaining popularity, one of the possible markets can include applications where ambient temperatures can be subzero. This paper aims to show the feasibility of using the grid described previously to generate turbulence and pre-heat the air, simultaneously, to avoid freezing conditions inside the cell. Four different designs were studied to achieve higher convective heat transfer while decreasing the surface temperature of the grid.

This paper is organized as follows: Section "Thermodynamic Balances and Streams" will present the thermodynamics calculations and assumptions of this research, "Computational Modelling" section will present the computational domain, the modelling equations, and the boundary conditions. The "Results and Discussion" section will present the results and an analysis of them. Finally, all the conclusions will be summarized in the "Conclusion" section.

Thermodynamic Calculations

The main goal of this study was to achieve a proper performance of the fuel cell while operating in freezing conditions. One of the most important inputs is the velocity of the air at the inlet of the cathode but also to know the operating voltage of the cell. Using the energy conservation principle, the energy balance can be written as:

$$\sum (H_i)_{in} = W_{el} + \sum (H_i)_{out} + Q \qquad [1]$$

Where, Q is the heat of the system, $(H_i)_j$ is the total enthalpy of the system, W_{el} is the electrical work of the fuel cell, and, due to this fact, it is possible to have it as a function of the current, $I_{cell,}$ and the cell voltage, V_{cell}:

$$W_{el} = V_{cell} \cdot I_{cell} \qquad [2]$$

A previous paper assumed an ideal gas behavior in order to calculate the enthalpy streams (1). This was an important assumption to combine both equations in the energy balance and, finally, calculating the cell voltage.

$$V_{cell} = \frac{1}{4F} \cdot (\zeta_{ca} - 1) \cdot \left(\overline{h_{O_2}}(T_{out}) - 8682 \frac{kJ}{kmol}\right)$$

$$+ \frac{1}{4F} \cdot 3.762 \cdot \zeta_{ca} \cdot \left(\overline{h_{N_2}}(T_{out}) - 8669 \frac{kJ}{kmol}\right)$$

$$+ \frac{1}{2F} \cdot (\zeta_{ca} - 1) \cdot \left(\overline{h_{H_2}}(T_{out}) - 8468 \frac{kJ}{kmol}\right) +$$

$$\left[\frac{RH \cdot \frac{p_{sat}(T)}{p_{total}}}{(1 - RH \cdot \frac{p_{sat}(T)}{p_{total}}} \cdot 4.762 \cdot \frac{\zeta_{ca}}{4F} + \frac{1}{2F}\right] \cdot$$

$$\left(-241.820 \frac{kJ}{kmole} + \overline{h}_{H_2O}(T_{out}) - 8468 \frac{kJ}{kmol}\right) \quad [3]$$

Where, F is the Faraday constant, T_{out} is the temperature of the system at the outlet, ζ_{ca} is the cathode stoichiometric ratio, p_{total} is the total pressure and, finally, p_{sat} is the saturation pressure.

With the goal of simplifying such equations, three important assumptions have to be considered. The system is adiabatic, the air at inlet is dry and the products of such reaction will be in the gas phase. Aiming to calculate the total enthalpy streams, the molar flow rate is needed as the sensible enthalpies and the enthalpies of formation.

So, the inlet molar streams, at the cathode side, of oxygen, nitrogen and water are given by the following equations, respectively (1)(8):

$$\dot{n}_{O_2,in} = \zeta_{ca} \frac{I}{4F} \quad [4]$$

$$\dot{n}_{N_2,in} = \frac{79}{21} \cdot \zeta_{ca} \frac{I}{4F} \quad [5]$$

$$\dot{n}_{H_2O,in} = RH_{in} \cdot \left(\frac{p_{sat}(T)}{p_{amb}} - RH_{in}\right)^{-1} \cdot 4.7619 \cdot \zeta_{ca} \frac{I}{4F} \quad [6]$$

Where the I, F, ζ_{ca}, RH_{in} , p_{amb} are the total current drawn from the fuel cell stack, the constant of Faraday, the stoichiometric flow ratio, is the relative humidity and, finally, the ambient pressure.

The saturation pressure is a function of the temperature and can be expressed by the equation of Antoine:

$$p_{sat}(T) = D \cdot e^{\left(A - \frac{B}{C+T}\right)} \quad [7]$$

In this equation, A, B and C are constants and D is a scalar to have the value in Pascal where A is 8.07131, B 1730.63, C is 233.426 and, finally, D is 133.233.

With respect to the anode side, the hydrogen molar flow rate is given by:

$$\dot{n}_{H_2,in} = \zeta_{an} \frac{I}{2F} \quad [8]$$

In this paper, the velocity at the cathode was calculated using the flow rate of the air and the assumption of ideal behavior. A detailed explanation can be found in (8) and the final equation is given as:

$$u_{in} = \zeta \frac{I}{4 \cdot F} \cdot A_{MEA} \cdot \frac{1}{x_{O_{2,in}}} \frac{R \cdot T_{in,ca}}{P_{in}} \frac{1}{A_{channel}} \quad [9]$$

This velocity, u_{in} is the velocity at the inlet of the cathode. However, as it will be shown in the section "Computational Modelling", $A_{channel}$ *is the* cross-sectional area of the channel before the cell itself is wider than the cathode cross-sectional area, A_{ca}. So, considering the fluid as incompressible the velocities can be related as:

$$u_{ch} = u_{in} \frac{A_{ch}}{A_{ca}} \quad [10]$$

Where u_{ch} is the velocity before the cathode inlet. In respect of the heated grid, the temperature difference across the grid was analyzed and the mass flow rate was calculated as:

$$\dot{m} = \rho \times u_{ch} \times A_{ca} \quad [11]$$

Previously, ρ is the density of the air. Multiplying the previous equation by the specific heat and the temperature difference, the heat input required is obtained, Q_{req}.

The volume of the grid, V_{grid}, is also a fundamental parameter to calculate the heat generation required. Finally, the heat generation uniformly distributed inside the turbulence grid is:

$$Q_{gen} = Q_{req}/V_{grid} \quad [12]$$

Computational Modelling

An overview of the computational domain and the inputs of the setup will be presented. As it was mentioned, the goal of setting a turbulence inducing grid before the cathode inlet was to increase the turbulence presented in the air flow and enhance the heat transfer rate between the cell and the air. A similar setup from [7] was used for the first simulations where a bipolar plate (BP), a gas diffusion layer (GDL) and a grid were modelled as solid cells and the remaining domain was modelled as fluid cells. An example of the computational domain is presented below:

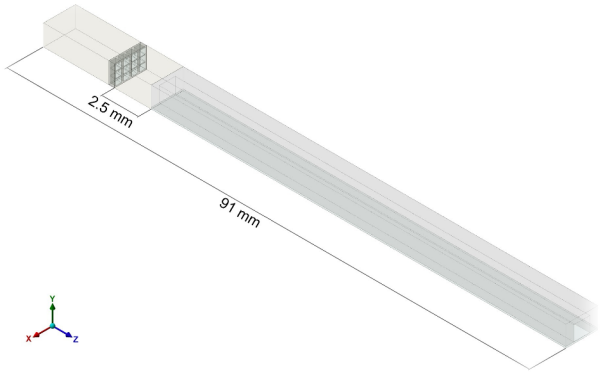

Figure 1. Computational domain used along the first simulations. Bipolar plate is represented as the light grey, gas diffusion layer as the dark grey and the grid was stablished to be at 2.5mm from the cathode inlet. However, to decrease the computational cost a symmetry plane Y-Z was used.

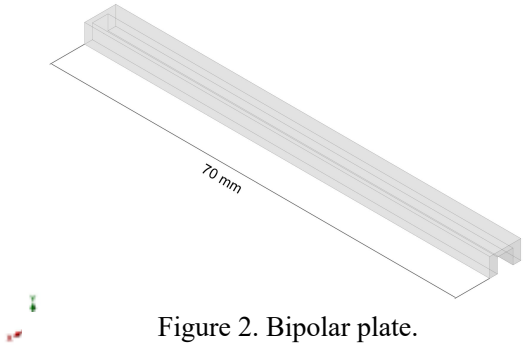

Figure 2. Bipolar plate.

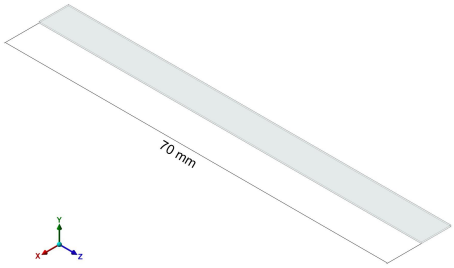

Figure 3. Gas diffusion layer.

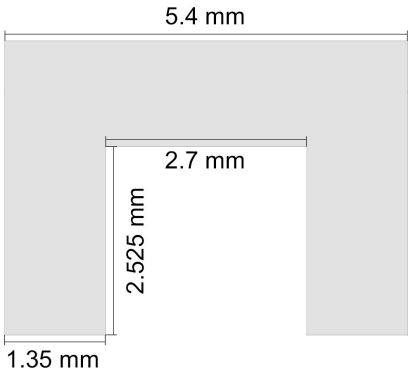

Figure 4. Front view of the bipolar plate.

Figure 5. Front view of the gas diffusion layer.

Table I. Overview of the material properties

Property	Bipolar plate	Gas diffusion layer
Density [kg/m^3]	1970	450
Specific Heat [J/(kg·K)]	720	900
Thermal Conductivity [W/(mK)]	20.5	1.7
Surface Roughness [m]	0	$1 \cdot 10^{-6}$

In this work, four different turbulence grids were studied. The main differences between these four grids are the number of pores (12 or 24) and the thickness of the grid (1 or 2mm).

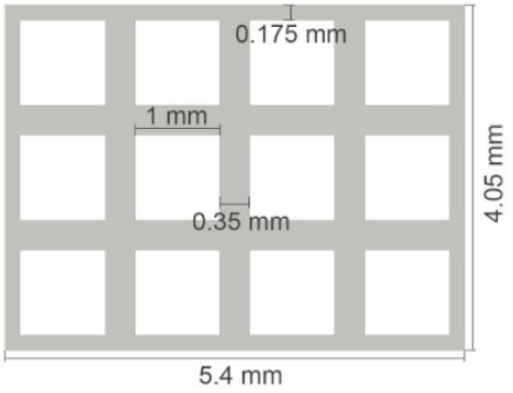

Figure 6. Grid geometry with 12 pores.

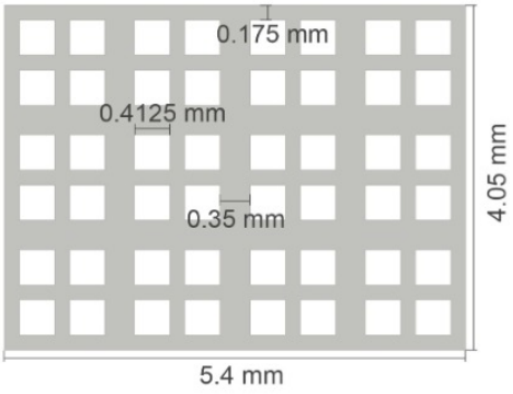

Figure 7. Grid geometry with 24 holes.

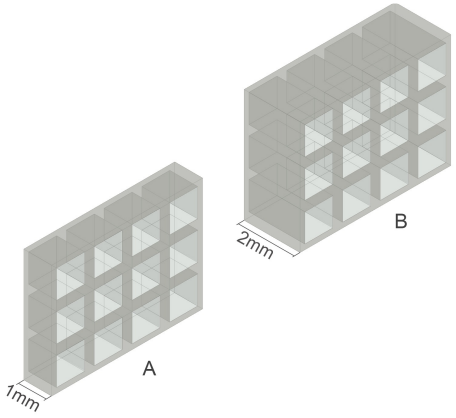

Figure 8. Shows the grid geometries with 12 pores and along with different depths.

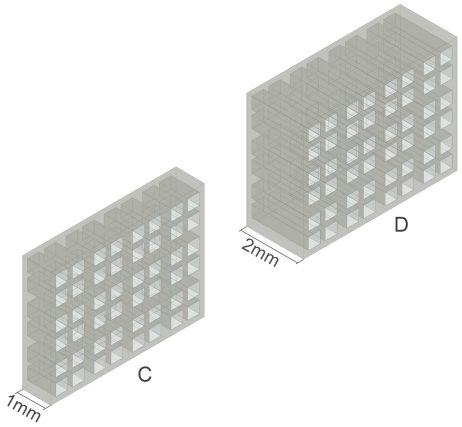

Figure 9. The grid geometries with the two different depths for the 24 pore grids.

The boundary conditions represent one of the most important parts when setting a computational fluid dynamic analysis. Bringing into play the equations presented on the previous section it was possible to define the velocity at the inlet and the temperature.

In addition, a constant heat flux was applied in the bottom of the gas diffusion layer where the catalyst layer would be. The heat flux is calculated out of an assumed cell voltage of 0.6V and a current density of 3850 A/m^2. Furthermore, the volume of the grid is a fundamental parameter to calculate the heat generation required. Finally, the boundary conditions are presented in the following table:

Table II. Overview of the boundary conditions

Location	Boundary Condition	Value
Inlet	Velocity	0.9557 m/s
Gas Diffusion Layer	Heat Flux	2587 W/m2
Rest of the domain	Symmetry	No flux

The inlet temperature of the air was varied from -20°C to 0°C in steps of 5°C, and the volumetric heat source inside the turbulence grid was calculated such that the air would be 5°C when entering the fuel cell channel. The result of these calculations would be the indicative temperature of the turbulence grid which in turn gives insight into the material requirement.

With regards to the equations used in this paper, the conservation of mass, momentum and energy were considered, respectively:

$$\frac{\partial \rho}{\partial t} + \nabla \cdot (\rho \mathbf{U}) = 0 \qquad [13]$$

$$\underbrace{\frac{\partial(\rho U_i)}{\partial t}}_{\text{Unsteady Term}} + \underbrace{\frac{\partial \rho U_i U_j}{\partial x_j}}_{\text{Convective Term}} = \underbrace{-\frac{\partial p}{\partial x_i}}_{\text{Pressure}} + \underbrace{\frac{\partial}{\partial x_j}\left(\mu \frac{\partial U_i}{\partial x_j}\right)}_{\text{Shear Stress}} + \underbrace{\frac{\partial\left(-\rho \overline{u_i' u_j'}\right)}{\partial x_j}}_{\text{Reynolds Stress}} \qquad [14]$$

$$\underbrace{\frac{\partial\left(\rho c_p T\right)}{\partial t}}_{\text{Unsteady Term}} + \underbrace{\nabla \cdot \left(\rho c_p \mathbf{U} T\right)}_{\text{Convective Term}} = \underbrace{\nabla \cdot \left(\left(k + \frac{c_p \mu_t}{Pr_t}\right) \nabla T\right)}_{\text{Diffusive Term}} + \underbrace{S}_{\text{Heat Source}} \qquad [15]$$

In order to solve the term called “Reynolds Stresses”, the Reynolds Stress model was used in this paper. This approach directly computes all the individual components of the Reynolds stresses from their transport equations. This approach will have seven extra equations to be solved [9].

Results and Discussion

In this section, the results obtained from the simulations will be presented. All the previous four grids were considered, and this section will present the results of each grid separately. Although, the aim of this paper was to study the performance of all grids, grid A was used a benchmark since it was already used in previous papers. To study all the possible performances of each grid, five different steady simulations were developed where the temperature difference between the inlet of the cathode and the ambient temperature was changed.

The calculated heating power of the turbulence grid results out of the energy requirement to heat up the incoming air stream to the desired inlet temperature, here 5°C.

This must be compared to the electric power that the fuel cell can produce. Typically, air-cooled fuel cells have a power density in the range of 0.25 W/cm^2 [5]. From above we see that the active area of the fuel cell section in the current case is 0.54 cm by 7 cm which is 3.78 cm^2. Hence the fuel cell section produces close to 1 W.

Grid A

As it was mentioned, Grid A acted as the benchmark of this paper. An important detail to have a better understanding of the results is the volume of each grid and in Grid A case the volume is 4.935 mm^3. It is understood that the grid temperature is a result of these calculations, and we are trying to gain insight into the required heat input and grid materials.

Table III. Resulting grid surface temperatures for grid dimension A in the CFD simulations.

Inlet air velocity[m/s]	Heat input [W]	ΔT across the grid	Grid temperature [ºC]
0.9557	0.3268	25 ºC	1511 ºC
0.9557	0.2615	20 ºC	1223 ºC
0.9557	0.1961	15 ºC	928 ºC
0.9557	0.1307	10 ºC	626 ºC
0.9557	0.0654	5 ºC	319 ºC

The volume of Grid A is relatively small and, when compared to the other grids, it is the smallest one. It was possible to notice, the resulting grid temperature was very high and peaked at a temperature of 1511 ºC. This resulting temperature is out of the range of the other components' temperature and fluids. It is possible to notice in the figure 4, the preheating of the incoming air, having a temperature of -10 ºC. As it can be seen, the cold air reaches the grid and as it flows through it gets heated up via convection and reaches an approximate value of 5 ºC after the grid.

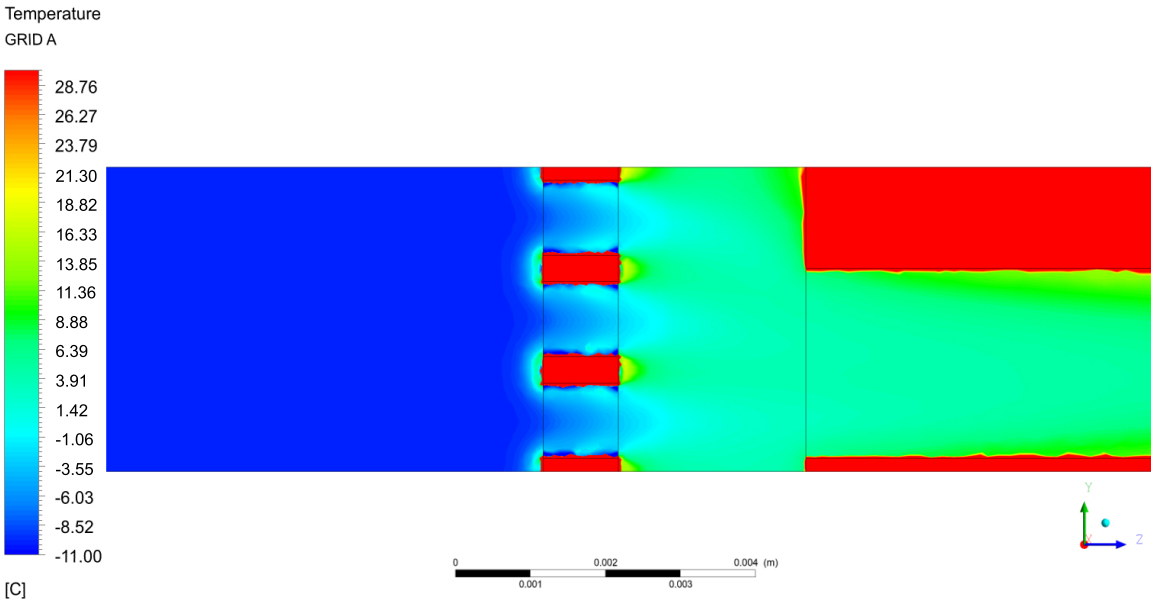

Figure 10. The temperature profile of the air as it flows through the turbulence inducing Grid A. Note that the scale of this picture is up to 29 ºC in order to be possible to see the different temperatures as long as the air flows through the pores. The flow is from left to right.

Grid B

As it is shown in figure 2, the Grid B has the same number of pores as Grid A. However, its width is increased to 2 cm. With this change, the surface area between the fluid and the solid surface is higher, increasing the heat transfer between the two regions. The temperatures of the surface of the grid are shown in the table below:

Table IV. Resulting grid surface temperatures for grid dimension B in the CFD simulations.

Inlet air velocity[m/s]	Heat input [W]	ΔT across the grid	Grid temperature [ºC]
0.9557	0.3268	25 ºC	863 ºC
0.9557	0.2615	20 ºC	699 ºC
0.9557	0.1961	15 ºC	531 ºC
0.9557	0.1307	10 ºC	359 ºC
0.9557	0.0654	5 ºC	184 ºC

The surface temperatures are lower than the temperatures of Grid A as it can be seen in Table V. However, the temperatures of the surface of the grid are still too high. The aim of this project was to have a maximum grid surface temperature of around 200 – 300 ºC.

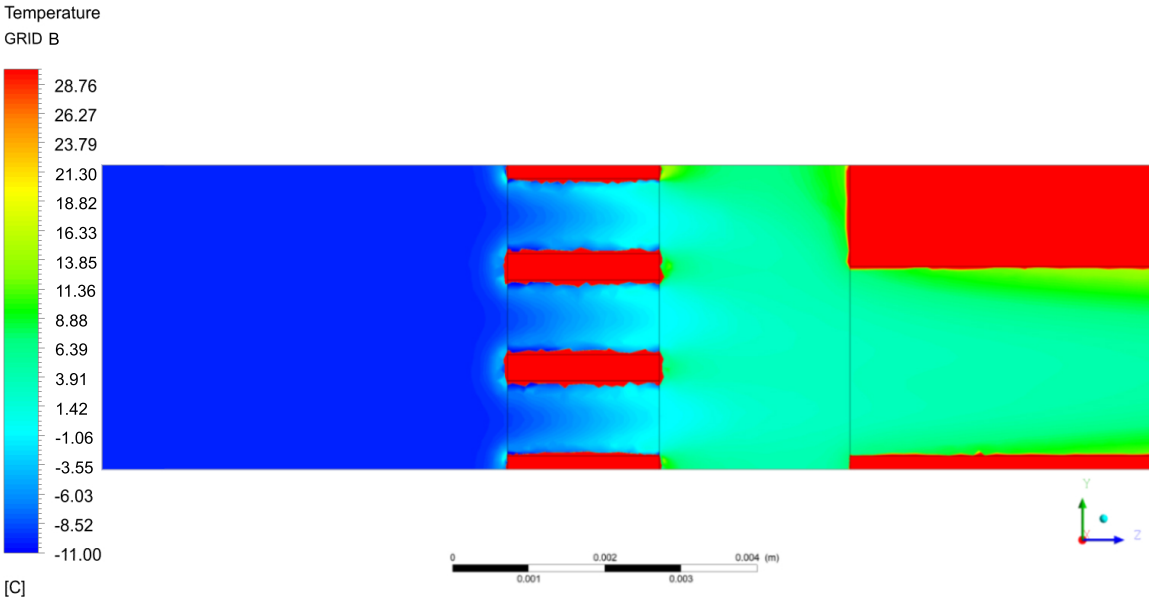

Figure 11. The temperature profile of the air as it flows through the turbulence inducing Grid B. The incoming air temperature was set to -10 ºC. The flow is from left to right.

Grid C

The main difference between Grid C versus Grid A and Grid B is the number of pores and the width, respectively. However, these differences increased the volume when looking to Grid A, the same did not happen when comparing to Grid B. So, it was possible to expect to have higher surface temperatures than the previous grid. The following table will show the different results of all five steady state simulations done with Grid C:

Table V. Resulting grid surface temperatures for grid dimension C in the CFD simulations.

Inlet air velocity[m/s]	Heat input [W]	ΔT across the grid	Grid temperature [ºC]
0.9557	0.3268	25 ºC	982 ºC
0.9557	0.2615	20 ºC	799 ºC
0.9557	0.1961	15 ºC	608 ºC
0.9557	0.1307	10 ºC	412 ºC
0.9557	0.0654	5 ºC	211 ºC

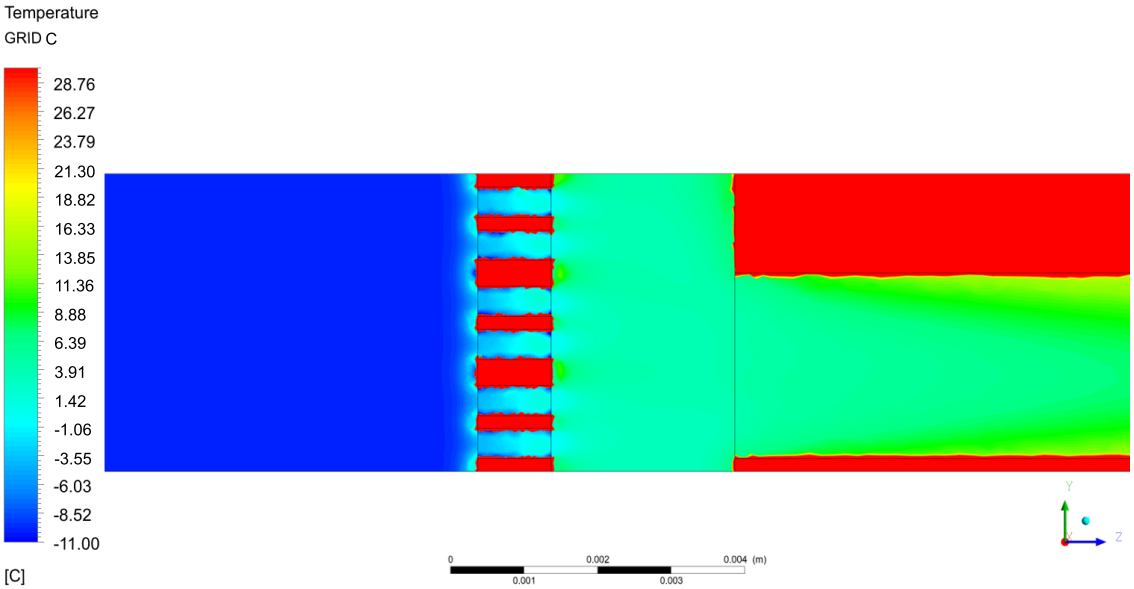

Figure 12. The temperature profile of the air as it flows through the turbulence inducing Grid C. The incoming air temperature was set to -10 ºC. The flow is from left to right.

Grid D

Finally, Grid D was the one after the designing stage where the promising results were expected since with 24 pores and 2 mm of width, its volume would be the biggest one. This is a temperature decrease of 580 ºC, when comparing to the grid surface temperature of grid A considering the same temperature difference across the grid.

Table VI. Resulting grid surface temperatures for grid dimension D in the CFD simulations.

Inlet air velocity[m/s]	Heat input [W]	ΔT across the grid	Grid temperature [ºC]
0.9557	0.3268	25 ºC	562 ºC
0.9557	0.2615	20 ºC	472 ºC
0.9557	0.1961	15 ºC	348 ºC
0.9557	0.1307	10 ºC	236 ºC
0.9557	0.0654	5 ºC	122 ºC

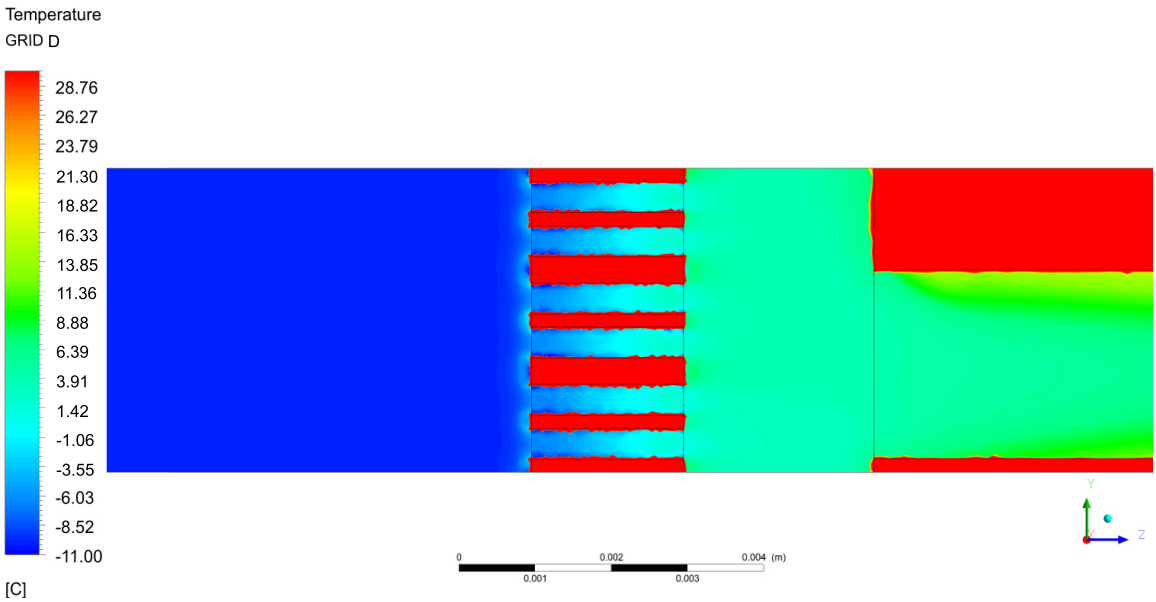

Figure 13. The temperature profile of the air as it flows through the turbulence inducing Grid D. The incoming air temperature was set to -10 ºC.

As it was possible to notice Grid D presented interesting results even when the ambient temperature was set to -15 ºC, achieving a surface temperature of 348 ºC. However, the amount of energy required from the grid to heat up the air was also analyzed. The table below illustrates the turbulence inducing grid power used when compared to the fuel cell power:

Table VII. Grid Power used compared to the fuel cell power generated.

Fuel Cell Power [W]	Grid Heat [W]	ΔT Across Grid	Grid heat/Fuel cell power (%)
0.8732	0.6536	25 ºC	74.85
0.8732	0.523	20 ºC	59.89
0.8732	0.3922	15 ºC	44.92
0.8732	0.2614	10 ºC	29.94
0.8732	0.1308	5 ºC	14.98

Where the fuel cell power was calculated according to the voltage obtained using the equation 3, a current density of 0.3850 A/cm^2 and the area of the gas diffusion layer. The percentage of power used by the heated turbulence inducing grid is the heat required by the grid over the power generated by the fuel cell.

In summary, regarding placing a heated turbulence inducing grid in front of the cathode channel, showed good results when considering its feasibility and the surface temperature. However, when looking at the amount of power required from the turbulence inducing grid, it is possible to notice that only to heat up by 10 ºC, around 30% of the fuel cell power generated would be used by the grid. Finally, to avoid such consumption, a device such as a battery could be used as an auxiliary device. A problem further with such a stretched grid could be that it could act as a flow straightener rather than a turbulence inducer. It might therefore be preferrable to use a number of staggered grids of smaller size. This will be

investigated in the future. In addition, it would be interesting to see at which minimum temperature the air can enter the fuel cell while freezing conditions in the GDL are avoided.

Conclusions

In this work, we have studied, the feasibility of placing a heated turbulence inducing grid in front of the cathode channel under freezing conditions. It can be seen for such dimensions of the turbulence inducing grid, pre-heating the air from -10 ºC to 5 ºC will already originate a grid surface temperature of 348 ºC. It is less feasible to have such approach when considering even lower ambient temperatures due to high and unfeasible surfaces temperatures. As a first approach, it is possible to operate an air-cooled fuel cell at subzero conditions to a certain temperature range. However, this situation will affect the efficiency of the system since an additional consumption of power, around 25% to 35%, is required for secondary actions. A possible solution for such situation would be the integration of a small storage energy system which would provide the required power to the turbulence inducing grid, avoiding the use of the fuel cell power for such requirement.

References

[1] Berning, T.; Knudsen Kær, S. A Thermodynamic Analysis of an Air-Cooled Proton Exchange Membrane Fuel Cell Operated in Different Climate Regions. Energies 2020, 13. doi:10.3390/en13102611.

[2] Blue Wave Consulting. Global Fuel Cells Market Size, Share & Forecast 2027 | BlueWave.

[3] Sevjidsuren, G.; Uyanga, E.; Bumaa, B.; Temujin, E.; Altantsog, P.; Sangaa, D. Exergy analysis of 1.2 kW NexaTM fuel cell module; IntechOpen, 2012.

[4] Berning, T. A Numerical Investigation of Heat and Mass Transfer In Air-Cooled Proton Exchange Membrane Fuel Cells. Fluids Engineering Division Summer Meeting. American Society of Mechanical Engineers, 2019, Vol. 59032, p. V002T02A030.

[5] Shakhshir, S.A.; Gao, X.; Berning, T. An experimental study of the effect of a turbulence grid on the stack performance of an air-cooled proton exchange membrane fuel cell. Journal of Electrochemical Energy Conversion and Storage 2020, 17, 011006.

[6] Pløger, L.J.; Fallah, R.; Al Shakhshir, S.; Berning, T.; Gao, X. Improving the Performance of an Air-Cooled Fuel Cell Stack by a Turbulence Inducing Grid. ECS Transactions 2018, 86, 77.

[7] Lind, A.; Yin, C.; Berning, T. A Computational Fluid Dynamics Analysis of Heat Transfer in an Air-Cooled Proton Exchange Membrane Fuel Cell with Transient Boundary Conditions. ECS Transactions 2020, 98, 255.

[8] Barbir, F. PEM fuel cells: theory and practice; Academic press, 2012.

[9] Fluent, A.; et al. Ansys fluent theory guide. Ansys Inc., USA 2011, 15317, 724–746.